

A New Estimate of the Cutoff Value in the Bak-Sneppen Model

C. A. Fish¹, J. J. P. Veerman²

November 23, 2021

Abstract

We present evidence that the Bak-Sneppen model of evolution on N vertices requires N^3 iterates to reach equilibrium. This is substantially more than previous authors suggested (on the order of N^2). Based on that estimate, we present a novel algorithm inspired by previous rank-driven analyses of the model allowing for direct simulation of the model with populations of up to $N = 25600$ for $2 \cdot N^3$ iterations. These extensive simulations suggest a cutoff value of $x^* = 0.66692 \pm 0.00003$, a value slightly lower than previously estimated yet still distinctly above $2/3$. We also study how the cutoff values x_N^* at finite N approximate the conjectured value x^* at $N = \infty$. Assuming $x_N^* - x_\infty^* \sim N^{-\nu}$, we find that $\nu = 0.978 \pm 0.025$, which is significantly lower than previous estimates ($\nu \approx 1.4$).

We also present some evidence that the rank-driven analyses provide a correct simplification.

Keywords— Bak-Sneppen model, critical threshold, rank driven dynamical systems, discrete dynamical systems, self-organized criticality, one-dimensional cellular automata

1 Introduction

The Bak-Sneppen model (BS) is a discrete dynamical system defined as follows. Choose a population size $N \in \mathbb{N}$ and consider a cyclic graph with N nodes. Assign to each node a *fitness* value uniformly at random from $[0, 1] \subset \mathbb{R}$. Name these fitness values (x_1, x_2, \dots, x_N) so that x_N and x_1 are neighbors (i.e. $x_{N+1} := x_1$ and $x_0 := x_N$). At each time step, determine the node x_j with smallest fitness (the *weakest*) and replace both it and its neighbors x_{j-1} and x_{j+1} with fresh values chosen uniformly at random from $[0, 1]$ (we say the nodes have *mutated*).

Via this process, the weakest nodes are repeatedly eliminated in a way reminiscent of biological evolution. The mutation of nodes neighboring the weakest coarsely reflects the effects of disappearing species on nearby species. Bak and Sneppen in [1] suggest that this model has dynamic features also seen in biological evolution, namely “Self-organized criticality” (see also [5] for discussion of “punctuated equilibrium” and [2] for precise exploration of these features).

Observe that if the fitness of the weakest node x_j decreases in a mutation, then the new weakest is one of x_j , x_{j-1} or x_{j+1} . In any case x_j will mutate on the next time step. Thus there is an “upward pressure” counteracted by the fact that strong nodes are always at risk of being neighbors to the weakest. Indeed, it was shown in [11] that the mean of the (time) limiting distribution of fitnesses is bounded away from 1, as the population size $N \rightarrow \infty$ (see [15] for a survey of related results).

After an initial period during which overall fitness increases, the model reaches an equilibrium state with the vast majority of the values above a certain *cutoff value*. Computer simulations suggest that, for each N , the (time) limiting distribution of fitnesses is uniform on $[x_N^*, 1]$ for some cutoff x_N^* depending on N . Moreover, it appears that as $N \rightarrow \infty$, the sequence of cutoff values x_N^* approaches a limiting value close to $2/3$. This cutoff value x^* has been experimentally estimated as 0.66702 ± 0.00008 [6], 0.66702 ± 0.00003 [14], and 0.6672 ± 0.0002 [4]. It was shown in [12] that, under certain assumptions, the cutoff is strictly less than 0.75.

¹Fariborz Maseeh Department of Math and Statistics, Portland State University; cfish@pdx.edu

²Fariborz Maseeh Department of Math and Statistics, Portland State University; veerman@pdx.edu

We found that on the order of N^3 time steps are required to reach the equilibrium (see Figure 2 and Table 1). Since at each timestep the weakest node must be found (which takes $O(N)$ time), the overall naive runtime is $O(N^4)$. Thus it is computationally extremely intensive to estimate the cutoff using naive iteration of the model. Because the model doesn't lend itself to parallelization, it is difficult to find a quicker way to run reliable simulations. By making use of certain characteristics of the dynamics of the model (see next section), we nonetheless reduced the runtime for $2 \cdot N^3$ time steps to a little over $O(N^3)$. Using this method, we performed the largest simulation to date, namely $2 \cdot N^3$ time steps for $N = 25600$. In comparison, Garcia et al. [4] simulated $N = 8000$ and did only $O(N^2)$ time steps.

We found a cutoff value of $x^* = 0.66692 \pm 0.00003$, a value slightly (but significantly) lower than previously estimated yet still distinctly above $2/3$. The latter is relevant, because it implies (as suggested by [6]) that the mean-field theory proposed in [3] is too simplistic. We also studied how the cutoff values x_N^* at finite N approximate the conjectured value x^* at $N = \infty$. Assuming $x_N^* - x_\infty^* \sim N^{-\nu}$, we find that $\nu = 0.978 \pm 0.025$, which is significantly lower than previous estimates ($\nu \approx 1.4$).

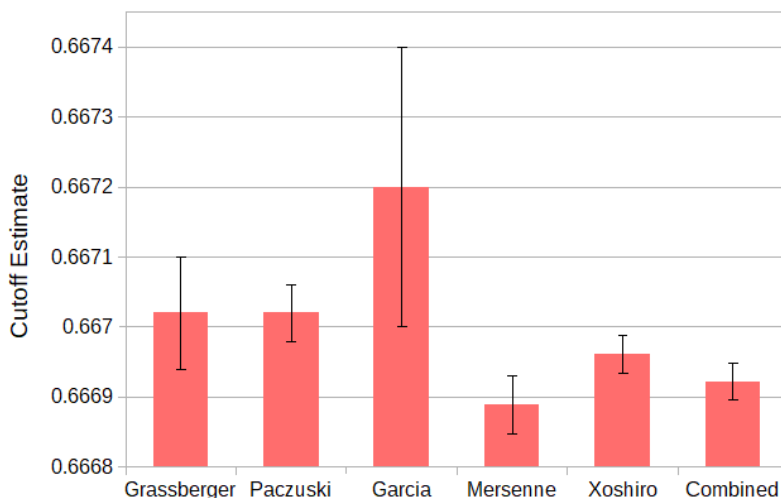


Figure 1: Comparison of our estimated cutoff values and those estimated by Grassberger [6], Paczuski [14], and Garcia [4]. As detailed in Section 2, we used two different RNGs (pseudorandom number generators) to obtain the cutoff value shown (“mersenne” and “xoshiro”) along with a cutoff value obtained by combining data from both RNGs.

Acknowledgement. We are grateful to Javier Prieto and Daniel Taylor-Rodriguez for their generous help with the statistics involved in this work.

2 Dynamical Characteristics of the Model

Onset of Equilibrium

Our approach is to iterate the model T_N times on N nodes until it reaches equilibrium. Once it reaches equilibrium, we iterate it another T_N times during which we perform our measurements. This way we insure that measurements are taken while the system is in equilibrium. Figure 2 provides evidence that equilibrium sets in after approximately $T_N = N^3$ iterates of the system. We found similar behavior for other values of N .

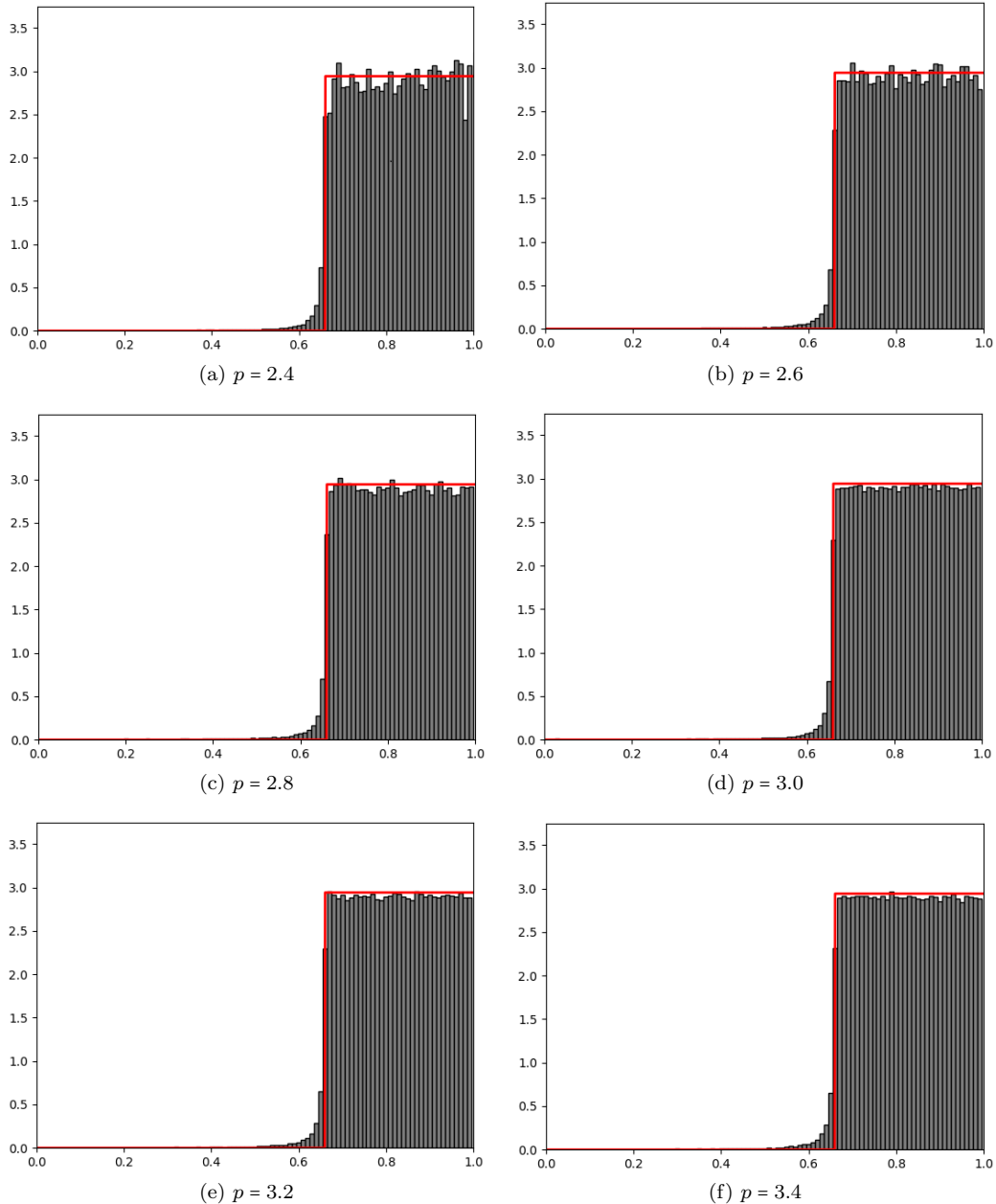


Figure 2: Histograms of fitness values for 500 population samples made after N^p time steps, for $N = 800$ and for $p \in \{2.4, 2.6, 2.8, 3.0, 3.2, 3.4\}$. These data suggest that the equilibrium is reached at $p \approx 3$. The uniform distribution on $(0.66, 1)$ has been overlaid. (Note that, above the cutoff, the empirical distribution is nearly entirely contained by the uniform distribution for $p \geq 3.0$.) In Table 1 we report the Cramér-von Mises statistics for these data.

Most Replacements Have Low Rank

We can order the values of the fitness by their *rank*. The lowest fitness is ranked “1”, the next lowest gets rank “2”, et cetera. The rank-driven analysis put forward in [7], [8], and [15] strongly suggests that the vast majority of mutations occur at the lowest ranks (when the nodes are ordered by fitness value). For example, Figure 3 illustrates the frequency at which the different ranks are replaced (after reaching the stationary distribution) for one simulation at $N = 800$. The overwhelming majority of

p	C.V.M. statistic
2.4	17.634
2.6	23.605
2.8	38.440
3.0	26.329
3.2	26.450
3.4	29.824

Table 1: We computed the Cramér-von Mises statistics (see e.g. [13]) on the empirical distribution of fitness values sampled 500 times after N^p time steps, for $N = 800$. The statistic gives a measure of distance between the empirical distribution of the sample and the uniform distribution on $(0.66, 1)$. As seen, the statistic is somewhat erratic for $p \in \{2.4, 2.6, 2.8\}$ but is more consistent for higher values, suggesting that at least $p \approx 3.0$ is needed.

replacements occur below rank 50. This motivates maintaining a *short list* containing only the lowest-ranked nodes. Mutated nodes may enter and leave the short list, where they stay “waiting” to be mutated. If the list grows too small, it is rebuilt by sorting the entire population. Keeping track only of relatively few lowest-ranked nodes on the short list allows us to find the position of the lowest ranked node without searching the whole population. The trick is to keep the list long enough so that we avoid sorting the entire population too often. This strategy allows us to iterate the model $2 \cdot N^3$ in barely over $O(N^3)$ time (see next section).

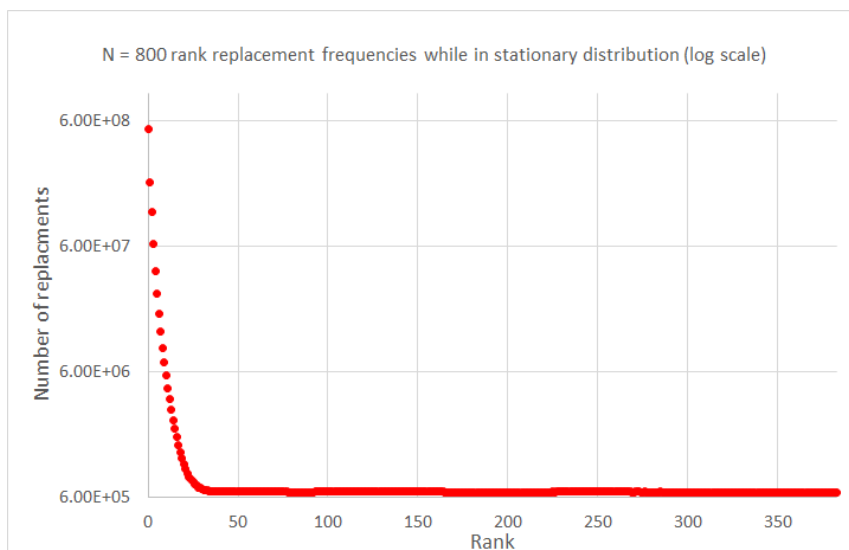


Figure 3: The frequency of mutation by rank found in one execution of the Bak-Sneppen model at $N = 800$. The minimum node (rank 0) is replaced the most often (since it is mutated every time step), and it appears that all but the lowest-ranked nodes are mutated rarely and at roughly equal frequency. (Note the logarithmic vertical axis.)

High Rank Replaced at Constant Rate

The rank-driven approach of [15] implies that the cutoff can be precisely determined if the sequence (indexed by N) of sequences of rank replacement frequencies $\{\alpha_i(N)\}_{i=1}^N$ form a so-called (p, q) -array. This is an array $\{\alpha_i(N)\}_{i=1}^N$ such that there exist p, q independent of N with

$$\sum_{i=0}^{K(N)} \alpha_i \leq p < \sum_{i=1}^{K(N)+1} \alpha_i \quad \text{and} \quad q = \sum_{i=K}^N \alpha_i.$$

for some $K(N) \in (1, N)$ depending on N such that $K(N) = o(N/\ln N)$. Furthermore, there must exist $\delta_i(N)$ and $\tilde{\alpha}(N)$ depending on N such that for ranks $i > K(N)$, the rank replacement frequencies α_i take the form $\tilde{\alpha}(N) + \delta_i(N)$ where $\max_{i > K(N)} |\delta_i(N)| = o(1/N)$ and $\tilde{\alpha}(N)$ is a constant – that is, the tail of the sequence of $\alpha_i(N)$ should increasingly flat as N tends to infinity. If the replacement frequencies $\{\alpha_i(N)\}$ form a (p, q) array, then one can prove [15] that the cutoff equals $\frac{p}{q}$.

Our data are consistent with the hypothesis that the sequences $\{\alpha_i(N)\}_{i=1}^N$ form a (p, q) -array, as illustrated in Figure 4. A more rigorous check is difficult in practice since the precise criterion for selecting $K(N)$ from data alone is unclear, and small errors in that choice amount to large differences in the estimate of x^* . Further investigation would indeed be useful.

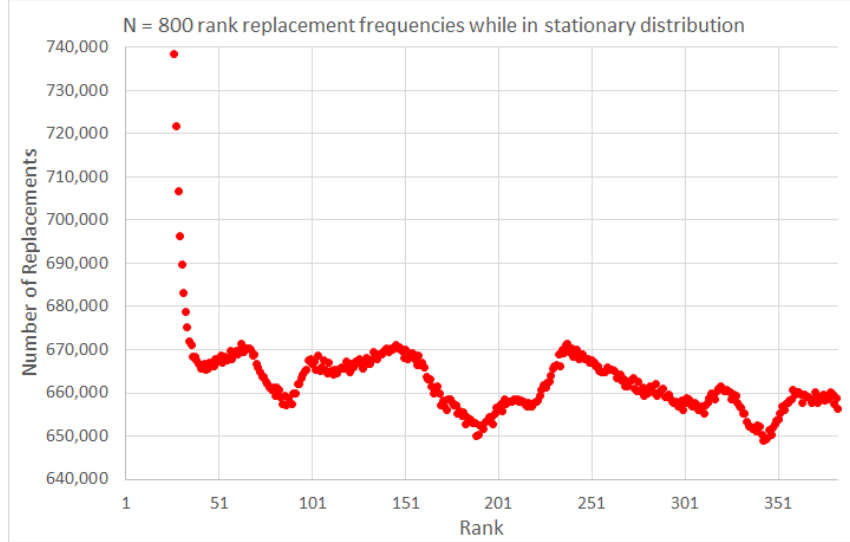


Figure 4: The frequency of mutation by rank found in one execution of the Bak-Sneppen model at $N = 800$, displaying only the vertical range $[640000, 740000]$. The data are very close to flat: the frequency beyond rank 50 deviates from flat by less than 2 out of 66 or $\pm 1.5\%$. Observe also that replacement rates appear to be continuous, perhaps even smooth (rather than random deviations from a mean).

Continuity of High Rank Replacement Rate

We also observe an unexpected continuity in the rank replacement frequencies (as in Figure 4); rank neighbors have correlated replacement frequencies. We propose the following heuristic explanation, making use of the fact that the distribution, $C(x)$, of the distance x between subsequent mutations is known (e.g. [1]) to follow a power law $C(x) = x^{-3.15 \pm 0.05}$. Let $R_t(x_i)$ be the rank of node x_i at time t , and let $P_t(r)$ be the probability that the node with rank r is mutated at time t . Suppose that at time t the weakest node is x_m , and so will mutate next. Consider some node x_k , distinct from x_m , x_{m-1} , and x_{m+1} . Prior to mutation, there is an approximate chance $p = C(d(x_m, x_k))$ that x_k will be mutated next³. Since x_k has rank $R_t(x_k)$, we can say $P_t(R_t(x_k))$ is also approximately p . After the mutation, at time $t + 1$, the new minimum is likely⁴ to be one of x_m , x_{m-1} , or x_{m+1} . If so, the chance that x_k is mutated next will be close to p , by the continuity of $C(x)$. Hence $P_{t+1}(R_{t+1}(x_k))$ is also close to p . However, $R_{t+1}(x_k)$ may differ from $R_t(x_k)$ due to the mutation, by at most 3. Thus, for $r = R_t(x_k) \pm 3$, we have $P_{t+1}(r) \approx P_t(R_t(x_k)) \approx p$, leading to an apparent approximate continuity in the graph of rank replacement frequencies.

³The value $d(x_m, x_k)$ being the minimal distance between x_m and x_k , i.e. the minimum of $|m - k|$ and $N - |m - k|$.

⁴The new minimum must be one of these three nodes unless all three increase in fitness as a result of the mutation.

3 Simulation Method

To simulate the model with our short list method, we used a multi-linked list data structure in C to keep track of the fitnesses, their *position neighbors*, and possibly their *rank neighbors*. That is, to represent the fitness value x_j , we create a node containing:

- a `double`⁵ approximating x_j
- a pointer to the node with fitness x_{j-1}
- a pointer to the node with fitness x_{j+1}
- (possibly) a pointer to the node with next largest fitness
- (possibly) a pointer to the node with next smallest fitness

Choosing some k depending on N , the simulation is initialized with only the $5k$ lowest-ranked nodes having pointers to their rank-neighbors. We also maintain pointers to the lowest and highest values on the short list.

To update the simulation once, the fitness of the lowest-ranked node x_j is replaced, along with the fitnesses of its two position neighbors x_{j-1} and x_{j+1} . It is then determined, for each of the three nodes x_j, x_{j-1}, x_{j+1} , whether they should or should not be on the short list. This is easy to check by comparing a new fitness value with the fitness of the highest-ranked node on the short list: the new fitness should be on the short list only if it is strictly less than this highest-ranked value. The neighbors x_{j-1} and x_{j+1} may or may not be on the short list already, and so may remain on, remain off, be inserted, or be removed. The rankings of all members of the short list are maintained appropriately as these operations are performed. If the length of the short list ever increases above $5k$, the ranks above $5k$ are simply “forgotten”. If it decreases to below $3k$, it is rebuilt by sorting the population. This last operation is expensive, but occurs infrequently (for example, in one simulation of 800 nodes lasting $800^3 = 5.12 \times 10^8$ iterations, the short list was rebuilt only 1419 times).

This method allows for simulation of large population values in a reasonable time. Our longest simulations ($N = 25600$) required approximately 45 days to complete⁶, while carrying out the same simulation using the naive method would take an estimated several thousand days.

Both the speed of the simulation and the frequency at which the short list is rebuilt will depend on the choice of k . We chose $k = 8$ for $N \in \{100, 200, 400\}$, $k = 16$ for $N \in \{800, 1600, 3200\}$, $k = 24$ for $N \in \{6400, 12800\}$, and $k = 32$ for $N = 25600$. These choices are likely not optimal and merit further investigation.

4 Estimation of the Cutoff

The cutoff for finite N

To estimate the cutoff value x_N^* for finite N , we performed simulations for various population values, using two separate pseudorandom number generators (RNGs) in order to mitigate bias: `xoshiro256+`

⁵a 64-bit floating-point type; see [9] for details

⁶on the Coeus HPC Cluster provided through the Portland Institute for Computational Science and Portland State University

(“Xoshiro”, see [16]) and MT19937-64 (“Mersenne twister”, see [10]). For each RNG we performed 20 simultaneous executions of the model at each of the population levels $N = 100 \cdot 2^i$ for $i \in \{0, \dots, 8\}$.

For each execution, we estimated the empirical cutoff x_N^* by the following method. First, iterate N^3 times to reach equilibrium. Then iterate N^3 times during which 500 snapshots are taken, one after each $N^3/500$ iterates. Collect these data into a histogram, in which the cutoff value is distinctly visible (see Figure 5). Since we expect the limiting fitness distribution

$$f(x) = \begin{cases} 0 & 0 \leq x < x^* \\ \frac{1}{1-x^*} & x^* \leq x \leq 1 \end{cases},$$

with $x \approx 2/3$, it is reasonable to define the transition point as the first index in the histogram at which the height exceeds 1.5. This gives the raw cutoff data summarized in Table 2. We also report “combined” values by pooling data from both RNGs before taking the mean and standard deviation.

i	0	1	2	3	4	5	6	7	8
N	100	200	400	800	1600	3200	6400	12800	25600
<u>Mers.</u>									
\bar{x}_i^*	0.60653	0.63885	0.65309	0.66033	0.66347	0.66512	0.66598	0.66637	0.66668
s_i	0.00916	0.00265	0.00144	0.00074	0.00025	0.00013	0.00005	0.00004	0.00003
<u>Xosh.</u>									
\bar{x}_i^*	0.60193	0.63981	0.65362	0.66031	0.66349	0.66502	0.66596	0.66635	0.66669
s_i	0.01197	0.00332	0.00128	0.00033	0.00024	0.00013	0.00006	0.00002	0.00002
<u>Comb.</u>									
\bar{x}_i^*	0.60423	0.63933	0.65335	0.66032	0.66346	0.66506	0.66597	0.66641	0.66668
s_i	0.01091	0.00304	0.00139	0.00057	0.00025	0.00014	0.00006	0.00003	0.00003

Table 2: The mean and standard deviation (over 20 executions) of the cutoff estimated via histogram, for each population value and for each RNG (Mersenne twister, Xoshiro) and for the combined data (found by pooling data from each RNG before taking the mean and standard deviation). Note that the population values are of the form $N = 100 \cdot 2^i$ for $i \in \{0, 1, 2, 3, 4, 5, 6, 7, 8\}$. Note also that these values do not correspond directly with Figure 1, as the latter values are obtained via the randomized data method described below.

Estimating x^*

Given these estimates for the values of x_N^* , we performed a statistical estimation of the cutoff at infinity $x^* = \lim_{N \rightarrow \infty} x_N^*$ using maximum likelihood estimation (MLE). Supposing that the values x_N^* follow the function

$$x_{100 \cdot 2^i}^* := f(i) = x^* - \kappa \lambda^i, \quad (1)$$

we used MLE to estimate the parameters x^* , κ , and λ . In particular, for $i \in \{0, \dots, 8\}$, let \bar{x}_i be the mean obtained via histogram and let s_i be the corresponding standard deviation (see Table 2). Then determine x^* , κ and λ that minimize

$$\chi^2(x^*, \kappa, \lambda) = \sum_{n=0}^8 \frac{(\bar{x}_i - f(i))^2}{s_i^2},$$

where $f(i)$ is given by (1). We minimized χ^2 via gradient method with a variable step⁷. This resulted in the estimated values for x^* , κ , and λ , seen in Table 3, for each RNG.

⁷In particular, we performed the backtracking line search method to determine the step size.

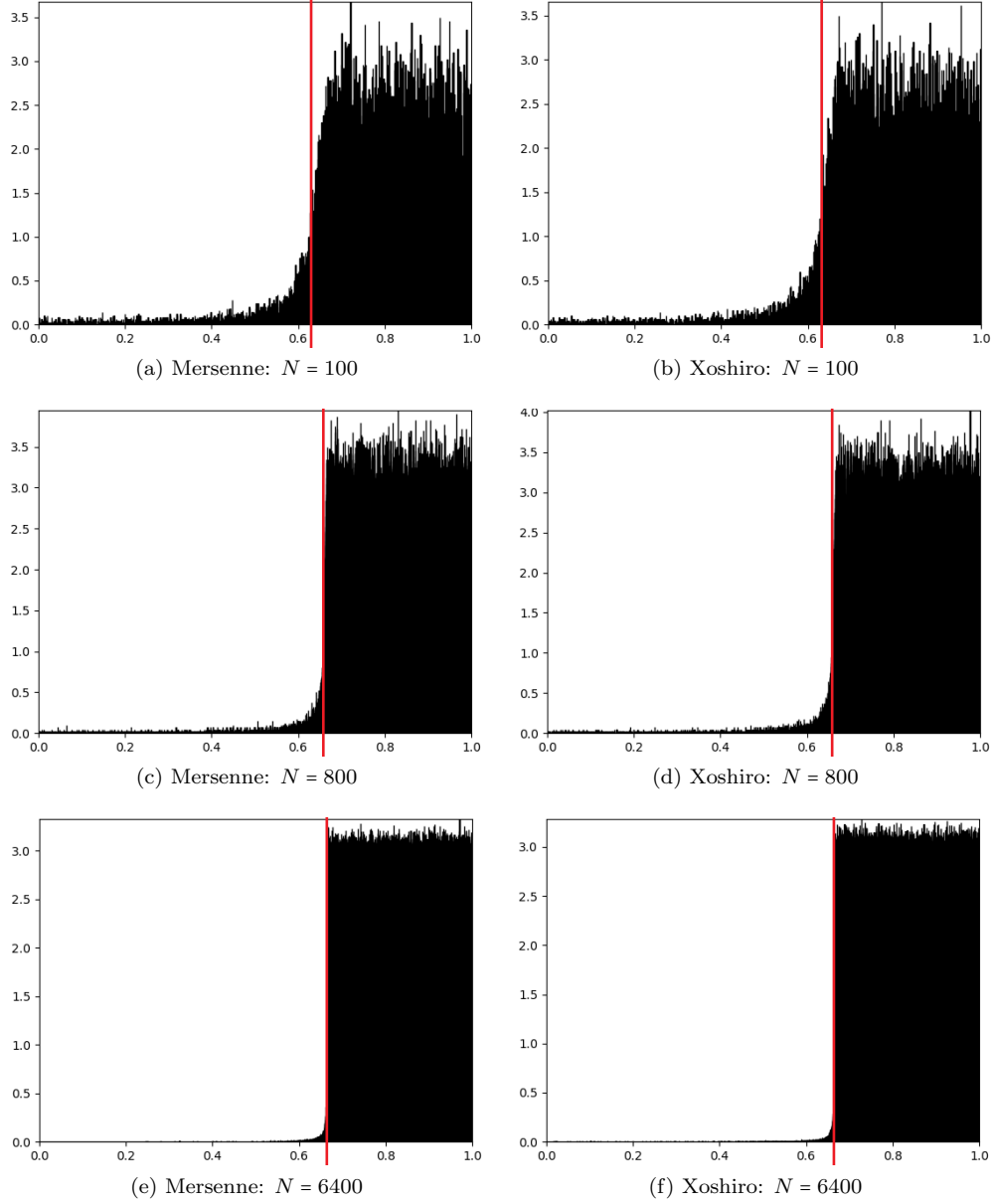


Figure 5: Histograms of fitness values for 500 population samples made after reaching the stationary distribution. The cutoff is distinct at the higher population counts, and is represented in the figure by a red line. Each histogram depicts one of 40 executions (20 per RNG). They are normalized to have area 1.

We take the x^* , κ , and λ associated with the combined data to be our best initial estimates. Beginning with these values, we determine our final estimates via the randomized data method described below.

Estimating errors on parameters

Having obtained an estimate for the cutoff, we estimated the error of our estimate using the following randomized data method. Initially, for each population level, and each RNG, we obtained an empirical cutoff value \bar{x}_i^* as a mean over 20 executions, and also obtained a standard deviation s_i . Supposing

	Mersenne	Xoshiro	Combined
x^*	0.66688	0.66697	0.66690
κ	0.05422	0.04442	0.05242
λ	0.50525	0.53743	0.51008
χ^2	3.9964	13.7271	2.6215

Table 3: Optimized parameters minimizing the χ^2 function. The minimum χ^2 value attained via these parameters is reported. Note that the relatively large χ^2 value for Xoshiro is due to the poorer fit at lower population values. However, the overall cutoff estimate is similar for all three RNGs.

that these data were drawn from a normal distribution \mathcal{N} with mean \bar{x}_i^* and standard deviation s_i , we drew 10 new samples from \mathcal{N} and performed the same MLE process described above, beginning with these artificial data. This process provided larger set of possible cutoff values, whose mean and standard deviation we report in Table 4. We take these means to be our best estimates for the Bak-Sneppen cutoff. We also report the mean and standard deviation of the associated values of λ , κ , and ν . See below for a discussion of ν , as well as Figure 6 illustrating models for $x^* - x_N^*$ fit with these mean parameters.

RNG	Mean x^*	\pm	Mean λ	\pm	Mean κ	\pm	Mean ν	\pm
Mersenne	0.66689	0.00004	0.51075	0.00631	0.05194	0.00284	0.969	0.018
Xoshiro	0.66696	0.00003	0.53091	0.01020	0.04597	0.00265	0.913	0.028
Combined	0.66692	0.00003	0.50758	0.00860	0.05393	0.00291	0.978	0.025

Table 4: Mean cutoff values and estimated standard deviation obtained via the randomized data method, for each RNG. Mean and standard deviation of associated λ , κ , and ν are also reported. To obtain the “combined” results, we pooled together empirical cutoff data from both RNGs before performing the randomization procedure. The estimated value of ν for the Xoshiro RNG is notably different from the others, which is consistent with the poorer fit of the Xoshiro data reported in Table 3. As before, we report the “Combined” data for our best estimates.

Estimating the exponent ν

To estimate ν in

$$x^* - x_N^* \propto N^{-\nu},$$

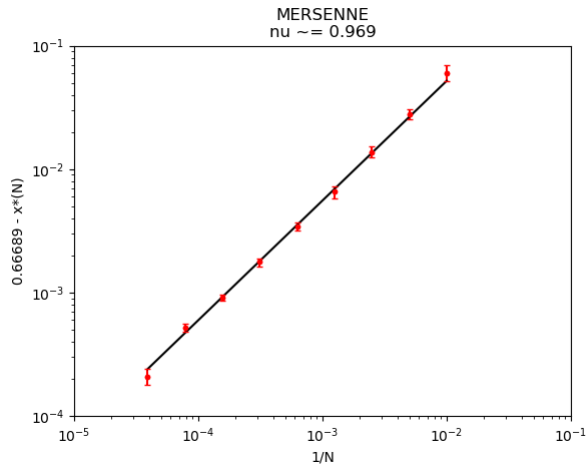
we need to rewrite this equation in terms of the parameters used so far. Recall that $x_{100 \cdot 2^i}^*$ is written as $f(i)$. So from (1), while noting that $i = \log_2(N/100)$, we obtain

$$x^* - x_N^* = \kappa \lambda^i = \kappa \lambda^{\log_2 N - \log_2 100} = (\kappa \lambda^{-\log_2 100}) \lambda^{\log_2 N} \propto N^{\ln \lambda / \ln 2},$$

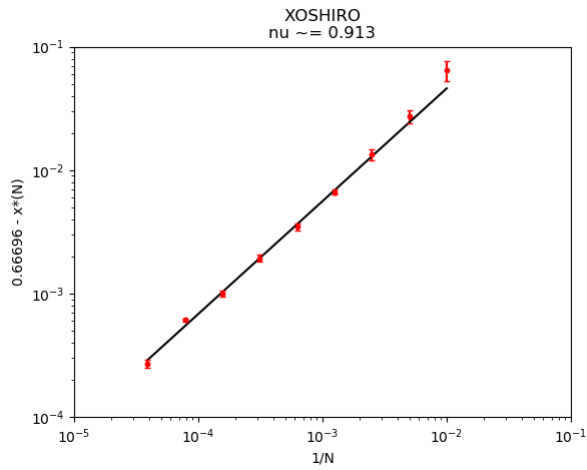
since $\log_2 N = \ln N / \ln 2$. Thus we obtain

$$\nu = -\ln \lambda / \ln 2.$$

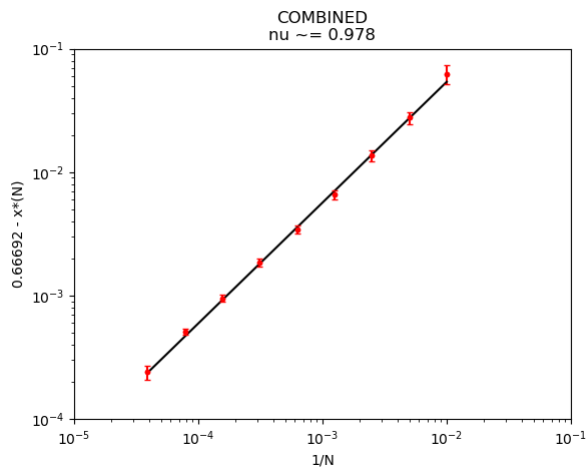
To get an idea, take the two values for λ in Table 3. This gives $\nu = 0.900$ and $\nu = 0.985$. Thus ν is particularly sensitive to variations in λ . We found an estimated range of values for κ and λ , and the corresponding range of values for ν , as reported in Table 4.



(a) Mersenne Twister



(b) Xoshiro



(c) Combined

Figure 6: Reformulating the model $x_{100,2^i}^* = f(i) = x^* - \kappa \lambda^i$ as a function of $\frac{1}{N}$, we can write $x^* - x_N^* = (\kappa \lambda^{-\log_2 100}) N^{-\nu}$, where $\nu = -\ln \lambda / \ln 2$. The figures show both the original x_N^* data alongside the model, using the mean parameters found in Table 4. Note that ν is the slope of the line, and is very close to 1. Indeed, our best estimated range of possible values $\nu = 0.978 \pm 0.025$ includes 1.

5 Conclusion

We summarize our overall results in Table 4 (see also Figure 1). Taking the “combined” value as our best estimate, it can be seen that our interval of possible values $[0.66689, 0.66695]$ has no overlap with Garcia’s interval $[0.66700, 0.66740]$, nor with Paczuski’s $[0.66698, 0.66710]$, while there is a small overlap with Grassberger’s $[0.66694, 0.66710]$. This suggests a true cutoff value lower than previously estimated but still significantly above $2/3$. We also estimate $\nu = 0.978 \pm 0.025$, differing significantly from previous estimates (e.g. a value of 1.4 is given in [4]). We note that $\nu = 1$ is included in this range, which may indicate the existence of a relationship $x^* - x_N^* \propto N^{-1}$, simpler than previously known.

Source	Estimated $x^* \pm$	Minimum	Maximum
Grassberger [6]	0.66702	0.00008	0.66694 0.66710
Paczuski [14]	0.66702	0.00004	0.66698 0.66706
Garcia [4]	0.66720	0.00020	0.66700 0.66740
Mersenne	0.66689	0.00004	0.66685 0.66693
Xoshiro	0.66696	0.00003	0.66693 0.66699
Combined	0.66692	0.00003	0.66689 0.66695

Table 5: Summary of our simulation results compared to cutoff values previously estimated. The minimum and maximum values (based on the reported error) are listed for ease of comparison.

6 Data availability statement

The data that support the findings of this study are available from the corresponding author, Cameron Fish, upon request. The simulation is written in C and the subsequent statistical analysis was performed with Python. The code for both can be found at <https://github.com/camafish/Bak-Sneppen>.

References

- [1] Per Bak and Kim Sneppen. Punctuated equilibrium and criticality in a simple model of evolution. *Physical Review Letters*, 71(24), 1993.
- [2] Jan de Boer, A. D. Jackson, and Tilo Wettig. Criticality in simple models of evolution. *Physical Review E*, 1994.
- [3] Henrik Flyvbjerg, Kim Sneppen, and Per Bak. Mean field theory for a simple model of evolution. *Phys. Rev. Lett.*, 71:4087–4090, Dec 1993.
- [4] G. J. M. Garcia and R. Dickman. On the thresholds, probability densities, and critical exponents of bak-sneppen-like models. *Physica A*, 342:164–170, 2004.
- [5] Stephen Jay Gould and Niles Eldredge. Punctuated equilibria: The tempo and mode of evolution reconsidered. *Paleobiology*, 3(2):115–151, 1977.
- [6] P. Grassberger. The bak-sneppen model for punctuated evolution. *Physics Letters A* 200, pages 277–282, 1995.
- [7] Michael Grinfeld, Philip A. Knight, and Andrew R. Wade. Bak-sneppen-type models and rank-driven processes. *Phys. Rev. E*, 84:041124, Oct 2011.

- [8] Michael Grinfeld, Philip A. Knight, and Andrew R. Wade. Rank-driven markov processes. *Journal of Statistical Physics*, 146(2):378–407, Oct 2011.
- [9] William Kahan. Lecture notes on the status of ieee standard 754 for binary floating-point arithmetic, October 1994.
- [10] Makoto Matsumoto and Takuji Nishimura. Mersenne twister: A 623-dimensionally equidistributed uniform pseudo-random number generator. *ACM Trans. Model. Comput. Simul.*, 8(1):3–30, January 1998.
- [11] R. Meester and Dmitri Znamenski. Limit behavior of the bak-sneppen evolution model. *Annals of Probability*, 31:1986–2002, 2003.
- [12] Ronal Meester and Dmitri Znamenski. Critical thresholds and the limit distribution in the bak-sneppen model. *Communications in Mathematical Physics*, 246:63–86, 2004.
- [13] M.S. Nikulin. Cramér-von mises test.
- [14] M. Paczuski, S. Maslov, and P. Bak. Avalanche dynamics in evolution, growth, and depinning models. *Physical Review E*, 53:414–443, 1996.
- [15] J. J. P. Veerman and Francisco J. Prieto. On rank driven dynamical systems. *Journal of Statistical Physics*, 156:455–472, 2014.
- [16] Sebastiano Vigna and David Blackman. xoshiro / xoroshiro generators and the prng shootout. <https://prng.di.unimi.it/>.